COBEM 2023 27TH INTERNATIONAL CONGRESS OF MECHANICAL ENGENEERING

ABCM Brazilian Society of Mechanical Sciences and Engineering
27th ABCM International Congress of Mechanical Engineering
December 04-08, 2023, Florianópolis-SC, Brazil

COB-2023-0761
EFFICIENCY OF THE REDUCER OF A BEVEL-GEARED MOTOR

Marina Baldissera de Souza
Gustavo Queiroz Fernandes
Daniel Martins
Universidade Federal de Santa Catarina, Departamento de Engenharia Mecânica, Centro Tecnológico, Campus Universitário – Trindade, 88040-900, Florianópolis - SC, Brazil
marina.bs@posgrad.ufsc.br - gustavo.fernandes@posgrad.ufsc.br - daniel.martins@ufsc.br

Andrea Piga Carboni
Universidade Federal de Santa Catarina, Departamento de Engenharias da Mobilidade, Campus Joinville, R. Dona Francisca, 8300 - Bloco U – Distrito Industrial, 89219-600, Joinville - SC, Brazil
andrea.piga@ufsc.br

Luís Paulo Laus
Universidade Tecnológica Federal do Paraná, Departamento de Mecânica, Av. Sete de Setembro, 3165 – Rebouças, 80230-901, Curitiba - PR, Brazil
laus@utfpr.edu.br

Abstract. *Bevel-geared motors are electric motors with a gear reducer connected to their output shaft, commonly used in industrial machinery requiring high torque. The efficiency of the reducer in a bevel-geared motor should be determined during its design phase, as the efficiency quantifies how effectively the bevel-geared motor is converting the electrical energy into mechanical power. This paper introduces an innovative approach to compute the efficiency of the reducer of a bevel-geared motor. A standard reducer's layout is considered, in which the reducer has two stages: the first corresponding to a pair of cylindrical gears, and the second composed of a pair of bevel gears with perpendicular shafts. The efficiency is determined via Davies' method, an analogy of Kirchhoff's voltage and current laws for solving the kinematics and statics of mechanisms, based on graph and screw theories. The total efficiency of the double-stage reducer obtained is equivalent to multiplying the individual stage efficiencies, the usual way to compute the efficiency of multi-stage transmissions. Thus, the paper's result demonstrates the effectiveness of the method. To the best of the authors' knowledge, it is the first time that graph and screw theories are applied to compute the efficiency of the reducer of a bevel-geared motor.*

Keywords: *Efficiency, bevel gear train, geared motor, transmission*

1. INTRODUCTION

Bevel gears have various applications in industry. They are usually found in bevel-geared motors, which are electric motors with a gear reducer connected to its output shaft, commonly used in industrial machinery requiring high torque. The standard layout of the reducer of a bevel-geared motor consists of two stages: the first corresponding to a pair of cylindrical gears, and the second composed of a pair of bevel gears with perpendicular shafts. Ideally, the mechanical efficiency of the reducer in a bevel-geared motor should be determined during its design phase, as the efficiency quantifies how effectively the bevel-geared motor is converting the electrical energy it consumes into mechanical power output. Unfortunately, academic works on the efficiency of bevel gear reducers are scarce and focus on experimentally determining the reducer performance. An equation for the efficiency of the reducer of a helical bevel-geared motor is experimentally obtained by Čarnogurská *et al.* (2014), by measuring the torque and speed at the inlet and outlet of the gearbox and applying dimensional analysis. Stockman *et al.* (2015) set up a measurement campaign to test a series of reducers of commercial electrical motors, aiming to determine the gearboxes' efficiency. Double and triple-stage reducers composed of bevel gears are among the 13 gearboxes whose efficiency was measured. No work proposing a method to estimate the mechanical efficiency of the reducer of a bevel-geared motor was found.

This paper aims to cover the need for more literature on the area by introducing an innovative approach to compute the mechanical efficiency of the reducer of a bevel-geared motor. The efficiency is determined via Davies' method, an analogy of Kirchhoff's voltage and current laws for solving the kinematics and statics of mechanisms, allying graph and screw theories (Laus *et al.*, 2012). Only meshing friction is considered in this paper, although nothing prevents including other causes of loss in future analyses. To the best of the authors' knowledge, it is the first time that graph and screw theories are applied to compute the efficiency of the reducer of a bevel-geared motor. Moreover, it is the first time that the Davies method is used to compute the efficiency of a gear train composed of cylindrical and bevel gears.

The paper is structured as follows. In Sec. 2, the use of the Davies method to compute the efficiency of gear trains is briefly explained. In Sec. 3, the overall efficiency of the reducer of a bevel-geared motor is determined via Davies' method. Finally, some conclusions are drawn in Sec. 4.

2. CALCULATING GEAR TRAINS' EFFICIENCY VIA DAVIES' METHOD

This section briefly explains the use of the Davies method for computing the mechanical efficiency of gear trains. More details are provided by Laus *et al.* (2012). In Davies' method, gear trains are represented by graphs, whose edges stand for the couplings and the vertices stand for the links. Once the graphs are defined, graph and screw theories are applied to build homogeneous linear systems for the motion and action analyses of the gear train. Velocities, forces, and moments are represented through screws. A screw \$ is defined by an instantaneous screw axis (ISA) given by a unit vector $\hat{s}$, the position vector $\vec{s}_0$ of one point belonging to the ISA, a pitch h, and a magnitude that quantifies the mechanical element described. When the magnitude is not specified, the screw is said to be normalized and is indicated by $\hat{\$}$. $\hat{s}$ and $\vec{s}_0$ are defined from a reference coordinate system O_{xyz}. The number of non-null elements of the screw gives the minimum order of the screw system λ, which defines the dimension of the space where the coupling is represented.

In the motion analysis, the screw is called twist, is represented by $\$^m$, and is composed of an angular velocity vector $\{r, s, t\}^T$ and a linear velocity vector $\{u, v, w\}^T$, according to Davies' notation (Davies, 2006). $\$^m$ is defined according to Eq. (1), where ϱ^m is the twist's magnitude:

$$\$^m = \varrho^m \left\{ \begin{array}{c} \hat{s} \\ \hdashline \vec{s}_0 \times \hat{s} + h\hat{s} \end{array} \right\} = \left\{ \begin{array}{c} r \\ s \\ t \\ \hdashline u \\ v \\ w \end{array} \right\} \tag{1}$$

The twists generate a homogeneous linear system through an adaptation of Kirchhoff's voltage law, resulting in Eq. (2), where $[\hat{M}_N]_{\lambda\nu \times F}$ is the network unit motion matrix, ν is the number of fundamental circuits of the graph, F is the gross degree of freedom, and $\vec{\psi}$ contains the twists' magnitudes.

$$\left[\hat{M}_N\right]_{\lambda\nu \times F} \left\{\vec{\psi}\right\}_{F \times 1} = \left[\vec{0}\right]_{\lambda\nu \times 1} \tag{2}$$

In the action analysis, screws are named wrenches, are indicated by $\$^a$, and consist of a moment vector $\{R, S, T\}^T$ and a force vector $\{U, V, W\}^T$, following the Davies' notation. $\$^a$ is determined via Eq. (3), where ϱ^a is the wrench's magnitude:

$$\$^a = \varrho^a \left\{ \begin{array}{c} \vec{s}_0 \times \hat{s} + h\hat{s} \\ \hdashline \hat{s} \end{array} \right\} = \left\{ \begin{array}{c} R \\ S \\ T \\ \hdashline U \\ V \\ W \end{array} \right\} \tag{3}$$

The wrenches compose a linear system via an analogy with Kirchhoff's current law, resulting in Eq. (4), where $[\hat{A}_N]_{\lambda\kappa \times C}$ is the network unit action matrix, κ is the number of fundamental cutsets of the graph, C is the gross degree of constraint, and $\vec{\Psi}$ contains the wrenches' magnitudes.

$$\left[\hat{A}_N\right]_{\lambda\kappa \times C} \left\{\vec{\Psi}\right\}_{C \times 1} = \left[\vec{0}\right]_{\lambda\kappa \times 1} \tag{4}$$

2.1 Screw systems for motion and action analyses of gear trains

Some simplifying hypotheses are proposed by Laus *et al.* (2012) to define the screw systems of the motion and action analyses and are elucidated in their work. Consider a reference coordinate system O_{xyz}. In cylindrical spur gears, the relative motions are angular velocities about axes parallel to the z-axis in the plane $x = 0$. Thus, the 2nd special 2-system of screws is adopted in the motion analysis, having $\lambda = 2$ (Hunt, 1978). In Davies' notation, the twists are spanned by the 2-system of screws $\{t, u\}$. So, the relative motions are represented by a twist with $h = 0$, ISA parallel to the z-axis, and angular speed magnitude t. The simplifying assumptions make that cylindrical spur gear trains transmit only forces parallel to the x-axis in the plane $z = 0$ and torques parallel to the z-axis. So, the 2nd special 2-system of screws is also adopted in the action analysis, represented by $\{T, U\}$ in Davies' notation and with dimension $\lambda = 2$. The forces are represented by wrenches with $h = 0$, ISA parallel to x-axis, and magnitude U. Wrenches representing torques have $h \to \infty$, ISA parallel to the z-axis, and magnitude T.

In straight bevel gears, the relative motions are rotations whose ISAs pass through the origin of O_{xyz} in the plane $x = 0$, which makes all twists belong to the 1st special 2-system of screws Hunt (1978). Following Davies' notation, the twists are spanned by the 2-system of screws $\{s, t\}$, with dimension $\lambda = 2$. Thus, the relative motions are given by twists with $h = 0$. When the twist's ISA is parallel to the y-axis, its angular speed magnitude is indicated by s. When the ISA is parallel to the z-axis, the angular speed magnitude is indicated by t. The simplifying hypotheses make that the actions transmitted by straight bevel gear trains are forces parallel to the x-axis and torques parallel to the plane $x = 0$. Thus, the wrenches belong to a 5th special 3-system of screws and can be spanned by the 3-system of screws $\{S, T; U\}$, with dimension $\lambda = 3$. The forces are represented by a wrench with $h = 0$, ISA parallel to x-axis, and magnitude U, while the torques are represented by wrenches with $h \to \infty$. When the torque wrench's ISA is parallel to the z-axis, its magnitude is given by T. When the torque wrench's ISA is parallel to the y-axis, the magnitude is indicated by S.

To both action and motion systems of screws have the same dimension λ, the motion system of screws is expanded from $\{s, t\}$ to $\{s, t; u\}$, the 4th special 3-system of screws. The last coordinate is null for all the twists. Consequently, the dimension of the action and motion systems of screws for straight bevel gear trains is $\lambda = 3$.

2.2 Power flow, efficiency, and power losses

The solutions of Eqs. (2) and (4) are used to compute the power flowing through the gear train. The power expended by a wrench $\$_j^a$ at a coupling j that allows a twist $\$_j^m$ to occur can be calculated as the inner product shown in Eq. (5):

$$\mathcal{P}_j = \$_j^a \cdot \$_j^m = rR + sS + tT + uU + vV + wW \tag{5}$$

If power enters the system through coupling j, $\mathcal{P}_j > 0$ Otherwise, $\mathcal{P}_j < 0$.

The gear train's overall efficiency is given by the ratio between the power $\mathcal{P}_{out}$ that leaves the gear train through the output and the power $\mathcal{P}_{in}$ that enters into the gear train via the input:

$$\eta = \frac{\mathcal{P}_{out}}{\mathcal{P}_{in}} \tag{6}$$

The effect of losses in gear trains is equivalent to a pure torque when the shafts are contained in the same plane (Laus *et al.*, 2012). In this paper, the meshing friction on the gear pairs is quantified by the Coulomb friction model. Assuming that power losses are not high enough to induce changes in the power flow direction, the meshing friction torque magnitude ϱ_L according to the Coulomb friction model is computed as:

$$\varrho_L = \zeta_i U_i \tag{7}$$

where U_i is the force along x direction transmitted by the gear pair i and ζ_i is the Coulomb friction factor of gear pair i, introduced by Laus (2011). ζ_i has unit of length to convert U_i into a torque. The losses that either occur at constant velocity or are independent of any motion are represented by ζ_i, which can be defined in terms of gears' pitch radii (r_d and r_f, the pitch radii of the driver gear and the follower gear, respectively) and the ordinary efficiency η_i of the gear pair. For cylindrical spur gears, ζ_i is calculated according to Eq. (8) (Souza *et al.*, 2017):

$$\zeta_i = \frac{r_d r_f (1 - \eta_i)}{r_d \pm \eta_i r_f} \tag{8}$$

The sign in the denominator of Eq. (8) depends on the meshing type: the plus sign is adopted for external meshing and the minus sign, for internal meshing.

For straight bevel gears with perpendicular axes and external meshing, ζ_i is calculated according to Eq. (9) (Souza, 2022):

$$\zeta_i = \frac{r_d r_f \sqrt{r_d^2 + r_f^2}(1 - \eta_i)}{r_d^2 + \eta_i r_f^2} \tag{9}$$

After calculating ζ_i, the equality $\text{sign}(\zeta_i) = -\text{sign}(U_i)\ \text{sign}(\varrho_i^m)$ must be checked, where ϱ_i^m is the magnitude of the angular speed of gear pair i. If the equality is not respected, ζ_i must be recalculated using η_i^{-1} instead of η_i in Eq. (8) or Eq. (9). This verification is done to confirm if the roles of driver/follower on the gear pair are correct.

3. EFFICIENCY OF THE DOUBLE-STAGE REDUCER OF A BEVEL-GEARED MOTOR

A double-stage reducer of a bevel-geared motor is shown in Fig. 1. Figure1(a) shows the CAD model of the reducer and Fig. 1(b) shows its schematic representation. The reducer is composed of four links: a fixed link (link 0), a drive gear (link 1), a complex gear (link 2), and an output gear (link 3). In Fig. 1(b), the drive gear is a cylindrical spur gear with pitch radius r_1, while the output gear is a straight bevel gear with pitch radius r_3. The cylindrical spur gear at the left side of the complex gear has pitch radius r_{2_a}, while the bevel gear at the right side has pitch radius r_{2_b}. The shafts of the bevel gear at the right side of gear 2 and the bevel gear 3 are perpendicular.

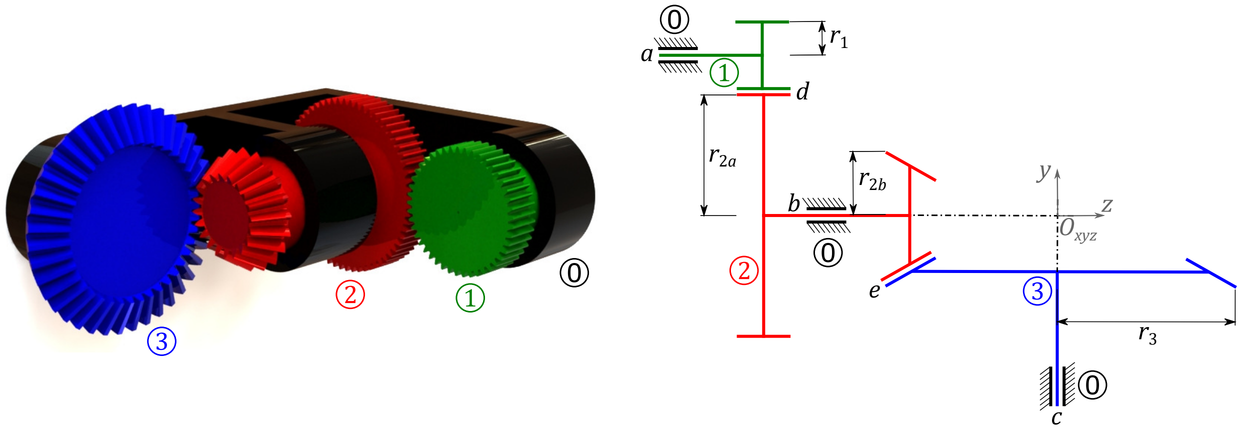

(a) (b)
Figure 1: (a) CAD model and (b) schematic representation of a bevel-geared motor reducer.

The couplings in Fig. 1(b) are labeled from a to e. Couplings a, b and c are revolute pairs, while couplings d and e are gear pairs. A reference frame O_{xyz} is attached to the intersection point of the axes of gears 2 and 3. The y-axis is parallel to the output gear's shaft, while the z-axis is parallel to the shafts of gears 1 and 2. The coupling graph of the gearbox presented in Fig. 1 is shown in Fig. 2(a).

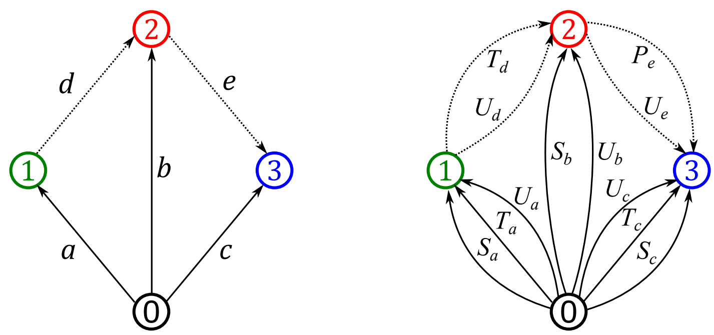

(a) (b)
Figure 2: Bevel geared motor's reducer: (a) coupling graph and (b) action graph.

3.1 Motion analysis

Before starting the motion analysis, the screw system for this particular case must be specified. As seen in Sec. 2.1, the 2-system of screws $\{t, u\}$ is adopted in the motion analysis of cylindrical spur gear trains. For straight bevel gear trains, the motion system of screws is $\{s, t, u\}$. Since the reducer is composed of bevel and cylindrical gears, the screw system adopted is $\{s, t, u\}$, as it comprises the system of both cases.

The rotation axes of couplings a, b, and d are parallel to the z-axis and their twists have magnitude t_a, t_b, and t_d, respectively, representing pure angular speeds. The twist of coupling c also represents a pure angular speed, but around y-axis, so its magnitude is s_c. The ISAs of the gear pair e is a straight line connecting the position of coupling e to the origin of O_{xyz}. The magnitude of the twist of coupling e is given by p_e. The motion parameters described herein are summarized in Tab. 1, where the ISA direction is given by the unit vector $\hat{s}$.

The twists are built through the data listed in Tab. 1 and Eq. (1), generating the network unit motion matrix $[\hat{M}_N]_{6\times5}$ shown in Eq. (10):

Table 1: Twists' parameters of the bevel geared motor

Coupling	Planar location		ISA direction	Twist's magnitude
	y	z	$\hat{s}$	
a	$r_{2_a}+r_1$	0	$\{0;0;1\}^T$	t_a
b	0	0	$\{0;0;1\}^T$	t_b
c	0	0	$\{0;1;0\}^T$	s_c
d	r_{2_a}	0	$\{0;0;1\}^T$	t_d
e	$-r_{2_b}$	$-r_3$	$\left\{0;-r_{2_b}/\sqrt{r_{2_b}^2+r_3^2};-r_3/\sqrt{r_{2_b}^2+r_3^2}\right\}^T$	p_e

$$[\hat{M}_N]_{6\times5} = \begin{array}{c} \begin{array}{ccccc} \hat{\$}_a^m & \hat{\$}_b^m & \hat{\$}_c^m & \hat{\$}_d^m & \hat{\$}_e^m \end{array} \\ \left[\begin{array}{ccccc} 0 & 0 & 0 & 0 & 0 \\ 1 & -1 & 0 & 1 & 0 \\ r_1+r_{2_a} & 0 & 0 & r_{2_a} & 0 \\ \hdashline 0 & 0 & -1 & 0 & -\frac{r_{2_b}}{\sqrt{{r_3}^2+{r_{2_b}}^2}} \\ 0 & 1 & 0 & 0 & -\frac{r_3}{\sqrt{{r_3}^2+{r_{2_b}}^2}} \\ 0 & 0 & 0 & 0 & 0 \end{array}\right] \end{array} \begin{array}{c} \\ s \\ t \\ u \\ s \\ t \\ u \end{array} \tag{10}$$

where the column labels on the top of $[\hat{M}_N]_{6\times5}$ indicate the normalized twist to which each column is related.

Equation (10) is the coefficient matrix of Eq. (2), which requires one primary variable to be solved since the reducer has 1 degree of freedom. Considering the speed of the drive gear (link 1) in relation to the fixed link as the primary variable, i.e. selecting t_a as the primary variable, the solution of the motion analysis is given by the vector $\{\vec{\psi}\}_{5\times1}$, which contains the twists' magnitudes. Equation (11) shows the transpose of $\{\vec{\psi}\}_{5\times1}$:

$$\{\vec{\psi}\}_{5\times1}^T = \begin{array}{c} \begin{array}{ccccc} t_a & t_b & s_c & t_d & p_e \end{array} \\ \left\{\begin{array}{ccccc} t_a & -t_a\frac{r_1}{r_{2_a}} & t_a\frac{r_1 r_{2_b}}{r_3 r_{2_a}} & -t_a\frac{(r_1+r_{2_a})}{r_{2_a}} & -t_a\frac{r_1\sqrt{{r_3}^2+{r_{2_b}}^2}}{r_3 r_{2_a}} \end{array}\right\} \end{array} \tag{11}$$

where the column labels indicate the magnitude to which the vector element corresponds.

The gear ratio of the bevel-geared motor reducer is obtained through the ratio between the input speed and output speed. Since coupling a is the input and coupling c the output, the gear ratio i_{BGM} of the reducer is:

$$i_{BGM} = \frac{t_a}{s_c} = \frac{r_3 r_{2_a}}{r_1 r_{2_b}} \tag{12}$$

where s_c comes from Eq. (11).

The solution shown in Eq. (11) leads to the motion matrix $[M]_{3\times5}$ for the reducer of the bevel-geared motor:

$$[M]_{3\times5} = t_a \begin{array}{c} \begin{array}{ccccc} \$_a^m & \$_b^m & \$_c^m & \$_d^m & \$_e^m \end{array} \\ \left[\begin{array}{ccccc} 0 & 0 & \frac{r_1 r_{2_b}}{r_3 r_{2_a}} & 0 & \frac{r_1 r_{2_b}}{r_3 r_{2_a}} \\ 1 & -\frac{r_1}{r_{2_a}} & 0 & -\frac{(r_1+r_{2_a})}{r_{2_a}} & \frac{r_1}{r_{2_a}} \\ r_1+r_{2_a} & 0 & 0 & -(r_1+r_{2_a}) & 0 \end{array}\right] \end{array} \begin{array}{c} \\ s \\ t \\ u \end{array} \tag{13}$$

where each column corresponds to a coupling's twist, as indicated by the columns' labels over $[M]_{3\times5}$.

3.2 Action analysis

The selection of the screw system for the action analysis follows the same reasoning used in the motion analysis. It is stated in Sec. 2.1 that the 2-system of screws $\{T, U\}$ is adopted in the action analysis of cylindrical spur gears. The action analysis of straight bevel gears requires the screw system $\{S, T, U\}$. So, in the action analysis of the reducer shown in Fig. 1, the system $\{S, T, U\}$ is adopted to compute the actions of both types of gear.

The action graph of the reducer is shown in Fig. 2(b). U_i, $i = a, b, c, d, e$ is the magnitude of the reaction forces, along x direction, transmitted by the couplings. T_a and S_c are magnitudes of the torque source and torque sink. S_a and S_b are the magnitudes of the reaction torques on y direction, while T_c is the reaction torque on z direction. T_d and P_e are the magnitudes of the friction torques on the gear couplings d and e. The wrenches representing friction torques have the same direction as the twists representing the motion of the respective coupling. So the friction torque on coupling d is parallel to z-axis and the friction torque on gear pair e is parallel to the line connecting the origin of O_{xyz} to the position of coupling e. Tab. 2 summarizes the data extracted from the screw-system definition and Fig. 1, such as the couplings' position and the wrenches' ISAs direction, given by the unit vector $\hat{s}$.

Table 2: Wrenches' parameters of the differential gearbox

Coupling	**Planar location**		**Action**	**ISA direction**	**Magnitude**
	y	z		$\hat{s}$	
a	$r_{r_a} + r_1$	0	Torque	$\{0;1;0\}^T$	S_a
			Torque	$\{0;0;1\}^T$	T_a
			Force	$\{1;0;0\}^T$	U_a
b	0	0	Torque	$\{0;1;0\}^T$	S_b
			Force	$\{1;0;0\}^T$	U_b
c	0	0	Torque	$\{0;1;0\}^T$	S_c
			Torque	$\{0;0;1\}^T$	T_c
			Force	$\{1;0;0\}^T$	U_c
d	r_{2_a}	0	Torque	$\{0;0;1\}^T$	T_d
			Force	$\{1;0;0\}^T$	U_d
e	$-r_{2_b}$	$-r_3$	Torque	$\left\{0; -r_{2_b}/\sqrt{r_{2_b}^2 + r_3^2}; -r_3/\sqrt{r_{2_b}^2 + r_3^2}\right\}^T$	P_e
			Force	$\{1;0;0\}^T$	U_e

The wrenches are built by applying the data shown Tab. 2 to Eq. (3) and create the network unit action matrix $[\hat{A}_N]_{9\times12}$. Two constitutive equations, defining the friction torques' magnitudes in the gear pairs, are appended to $[\hat{A}_N]_{9\times12}$ to generate an augmented action matrix $[D_A]_{11\times12}$ that is used as the coefficient matrix of Eq. (4). The constitutive equations are defined from the Coulomb friction model, given by Eq. (7), for gear pairs d and e:

$$T_d = \zeta_d U_d \tag{14}$$

$$P_e = \zeta_e U_e \tag{15}$$

where ζ_d and ζ_e are the Coulomb friction factors.

The resulting augmented action matrix $[D_A]_{11\times12}$ is:

$$[D_A]_{11\times12} = \begin{array}{cc}
\begin{array}{cccccccccccc} \hat{\$}^a_{S_a} & \hat{\$}^a_{T_a} & \hat{\$}^a_{U_a} & \hat{\$}^a_{S_b} & \hat{\$}^a_{U_b} & \hat{\$}^a_{S_c} & \hat{\$}^a_{T_c} & \hat{\$}^a_{U_c} & \hat{\$}^a_{T_d} & \hat{\$}^a_{U_d} & \hat{\$}^a_{P_e} & \hat{\$}^a_{U_e} \end{array} & \\
\left[\begin{array}{cccccccccccc}
1 & 0 & 0 & 0 & 0 & 0 & 0 & 0 & 0 & 0 & 0 & 0 \\
0 & 1 & -r_1 - r_{2_a} & 0 & 0 & 0 & 0 & 0 & -1 & r_{2_a} & 0 & 0 \\
0 & 0 & 1 & 0 & 0 & 0 & 0 & 0 & 0 & -1 & 0 & 0 \\
\hdashline
0 & 0 & 0 & 1 & 0 & 0 & 0 & 0 & 0 & 0 & \frac{r_{2_b}}{\sqrt{{r_3}^2+{r_{2_b}}^2}} & r_3 \\
0 & 0 & 0 & 0 & 0 & 0 & 0 & 0 & 1 & -r_{2_a} & \frac{r_3}{\sqrt{{r_3}^2+{r_{2_b}}^2}} & -r_{2_b} \\
0 & 0 & 0 & 0 & 1 & 0 & 0 & 0 & 0 & 1 & 0 & -1 \\
\hdashline
0 & 0 & 0 & 0 & 0 & 1 & 0 & 0 & 0 & 0 & -\frac{r_{2_b}}{\sqrt{{r_3}^2+{r_{2_b}}^2}} & -r_3 \\
0 & 0 & 0 & 0 & 0 & 0 & 1 & 0 & 0 & 0 & -\frac{r_3}{\sqrt{{r_3}^2+{r_{2_b}}^2}} & r_{2_b} \\
0 & 0 & 0 & 0 & 0 & 0 & 0 & 1 & 0 & 0 & 0 & 1 \\
\hdashline
0 & 0 & 0 & 0 & 0 & 0 & 0 & 0 & 1 & -\zeta_d & 0 & 0 \\
0 & 0 & 0 & 0 & 0 & 0 & 0 & 0 & 0 & 0 & 1 & -\zeta_e
\end{array}\right] &
\begin{array}{c} S \\ T \\ U \\ S \\ T \\ U \\ S \\ T \\ U \\ c.e \\ c.e. \end{array}
\end{array} \tag{16}$$

Using Eq. (16) as the coefficient matrix in Eq. (4) generates a homogeneous linear system that requires a single primary variable to be solved. The chosen primary variable is T_a, the torque source connected to the drive gear (link 1), resulting in a solution vector that leads to the condensed action matrix $[A]_{3\times 5}$ shown in Eq. (17):

$$[A]_{3\times 5} = \begin{array}{c} \begin{matrix} \$_a^a & \qquad\qquad \$_b^a & \qquad\qquad \$_c^a & \qquad\qquad \$_d^a & \qquad\qquad \$_e^a \end{matrix} \\ \left[\begin{matrix} 0 & \frac{\alpha_2\left(\alpha_1 r_3 + r_{2_b}\zeta_e\right)}{\alpha_1 r_{2_b} - r_3\zeta_e} & -\frac{\alpha_2\left(\alpha_1 r_3 + r_{2_b}\zeta_e\right)}{\alpha_1 r_{2_b} - r_3\zeta_e} & 0 & \frac{\alpha_2\left(\alpha_1 r_3 + r_{2_b}\zeta_e\right)}{\alpha_1 r_{2_b} - r_3\zeta_e} \\ -\alpha_2 & 0 & \alpha_2 & -\alpha_2 & -\alpha_2 \\ \frac{T_a}{r_1+\zeta_d} & -\frac{T_a\left(\alpha_1 r_{2_a} + \alpha_1 r_{2_b} - \alpha_1\zeta_d - r_3\zeta_e\right)}{\left(r_1+\zeta_d\right)\left(\alpha_1 r_{2_b} - r_3\zeta_e\right)} & \frac{\alpha_1\alpha_2}{\alpha_1 r_{2_b} - r_3\zeta_e} & \frac{T_a}{r_1+\zeta_d} & -\frac{\alpha_1\alpha_2}{\alpha_1 r_{2_b} - r_3\zeta_e} \end{matrix} \right] \end{array} \begin{matrix} S \\ T \\ U \end{matrix} \tag{17}$$

where $\alpha_1 = \sqrt{{r_3}^2 + {r_{2_b}}^2}$ and $\alpha_2 = T_a \frac{(r_{2_a} - \zeta_d)}{r_1 + \zeta_d}$. Each column of $[A]_{3\times 5}$ is a coupling's wrench.

Equations (13) and (17) are used to compute power flow and the overall efficiency of the reducer.

3.3 Power flow and efficiency

The twists composing the motion matrix shown in Eq. (13) and the wrenches of the action matrix in Eq. (17) are used to compute the power that enters or leaves the reducer through its input/output and the overall efficiency of the gearbox. Link 1, the drive gear, is the input link of the mechanism, so power enters into the reducer through coupling a and is calculated as:

$$\mathcal{P}_a = \$_a^m \cdot \$_a^a = T_a t_a \tag{18}$$

where $\$_a^m$ and $\$_a^a$ are the first columns of Eqs. (13) and (17), respectively. Since power enters the network through coupling a, $\mathcal{P}_a > 0$ and T_a and t_a have the same sign.

Link 3 is the output gear, thus, power leaves the reducer through coupling c and is determined as:

$$\mathcal{P}_c = \$_c^m \cdot \$_c^a = -T_a t_a \frac{r_1 r_{2_b}\left(r_{2_a} - \zeta_d\right)\left(r_3\sqrt{{r_3}^2 + {r_{2_b}}^2} + r_{2_b}\zeta_e\right)}{r_3 r_{2_a}\left(r_1 + \zeta_d\right)\left(r_{2_b}\sqrt{{r_3}^2 + {r_{2_b}}^2} - r_3\zeta_e\right)} \tag{19}$$

where $\$_c^m$ and $\$_c^a$ are the third columns of Eqs. (13) and (17), respectively. The output power $\mathcal{P}_c$ is negative as $T_a t_a > 0$ and $r_{2_a} > \zeta_d$ in practice, what is coherent, since coupling c is the reducer's output.

The reducer's overall efficiency η is the ratio between output and input power and is calculated using Eq. (6):

$$\eta = -\frac{\mathcal{P}_c}{\mathcal{P}_a} = \frac{r_1 r_{2_b}\left(r_{2_a} - \zeta_d\right)\left(r_3\sqrt{{r_3}^2 + {r_{2_b}}^2} + r_{2_b}\zeta_e\right)}{r_3 r_{2_a}\left(r_1 + \zeta_d\right)\left(r_{2_b}\sqrt{{r_3}^2 + {r_{2_b}}^2} - r_3\zeta_e\right)} \tag{20}$$

where $\mathcal{P}_a$ and $\mathcal{P}_c$ come from Eqs. (18) and (19), respectively.

The Coulomb friction factors ζ_d and ζ_e are computed via different equations. Coupling d connects two cylindrical gears, so Eq. (8) is used to compute ζ_d. Equation (9) is used to compute ζ_e, as the gear pair e connects two straight bevel gears with perpendicular axes. Since coupling a is assumed as the input, so $r_d = r_1$ and $r_f = r_{2_a}$ in Eq. (8):

$$\zeta_d = \frac{r_1 r_{2_a}(1 - \eta_{eg})}{r_1 + \eta_{eg} r_{2_a}} \tag{21}$$

where η_{eg} is the ordinary efficiency of a spur gear pair with external meshing and can assume the value of 0.98 (Glover, 1965). The plus sign is adopted in the denominator of Eq. (21) as coupling d is a gear pair with external meshing.

For coupling e, the right side of the complex gear 2 is the driver gear and the output gear 3 is the follower gear of coupling e. However, Souza (2022) deduced Eq. (9) using the simple bevel gear train shown in Fig. 3. Note that gear 2 is at the right side of O_{xyz} in Fig. 3, so the z coordinate of coupling c is positive.

In Fig. 1(b), the right side of gear 2 is at the left of O_{xyz}, so the z coordinate of coupling e is negative, as indicated in Tabs. 1 and 2. Therefore, the negative sign of the z coordinate of coupling e must be compensated, so $r_d = r_{2_b}$ and $r_f = -r_3$ in Eq. (9), leading to:

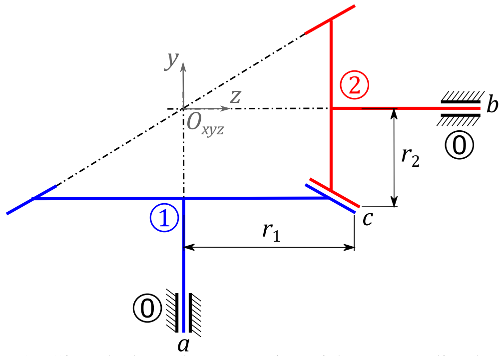

Figure 3: Simple bevel gear train with perpendicular axes.

$$\zeta_e = -\frac{r_{2_b} r_3 \sqrt{r_{2_b}^2 + r_3^2}(1-\eta_{bev})}{r_{2_b}^2 + \eta_{bev} r_3^2} \tag{22}$$

where η_{bev} is the ordinary efficiency of a straight bevel gear pair with perpendicular axes and η_{bev} can assume a value of 0.98 (Pathak *et al.*, 2016).

Replacing ζ_d by Eq. (21) and ζ_e by Eq. (22) in Eq. (20) gives Eq. (23):

$$\eta = \eta_{eg}\eta_{bev} \tag{23}$$

By inspecting Eq. (23), it can be noted that the efficiency of the bevel geared motor's reducer depends exclusively on the ordinary efficiencies when only meshing friction is considered. The overall efficiency of the double-stage reducer obtained through Davies' method and shown in Eq. (23) is equivalent to the result generated by multiplying the individual stage efficiencies, the usual technique to compute the efficiency of multi-stage transmissions (Bartlett *et al.*, 2018). Thus, the paper's result demonstrates the effectiveness of the method.

The outcome shown in Eq. (23) may seem obvious for experienced engineers, but the simplicity of the result is due to the fact that meshing friction is the single cause of loss considered in this paper. Although gearing losses constitute a substantial proportion of total power loss in industrial gearboxes, accounting for 50% to 70% of the losses (Čarnogurská *et al.*, 2014), other notable causes of loss are bearing and seal friction, swirling oil, and ventilation. When provided with a suitable friction model, the Davies method enables the incorporation of multiple loss causes simultaneously into the efficiency calculation. By taking into account these additional causes of loss, the resulting equation for the efficiency of the reducer of the bevel geared-motor may not be as self-evident as Eq. (23).

4. CONCLUSIONS

This paper proposed an innovative approach to determine the efficiency of multi-stage reducers of bevel-geared motors in the design phase, instead of estimating experimentally the efficiency. The approach consists of applying the Davies method to generate an analytical expression for the mechanical efficiency of the gearbox. A double-stage reducer, in which the first stage is composed of spur cylindrical gears and the second stage consists of a pair of straight bevel gears, is the case study of this paper.

The overall efficiency determined via Davies' method for the case study is equivalent to expressions found in the literature on power transmission. Therefore, this paper's results prove that the Davies method is a suitable tool to compute the efficiency of gear trains composed of different types of gears and can be applied to reducers with more complex geometries.

Future works include incorporating other causes of loss, such as bearing friction, to estimate the efficiency of the double-stage reducer shown in Fig. 1(a), and calculating the efficiency of gearboxes composed of cylindrical and bevel gears with epicyclic gearing.

5. ACKNOWLEDGEMENTS

This work was funded by the Coordenação de Aperfeiçoamento de Pessoal de Nível Superior - Brasil (CAPES) - Finance Code 001 and by the Conselho Nacional de Desenvolvimento Científico e Tecnológico (CNPq) [grant number 383653/2022-3].

6. REFERENCES

Bartlett, H.L., Lawson, B.E. and Goldfarb, M., 2018. "On the design of power gear trains: Insight regarding number of stages and their respective ratios". *PloS one*, Vol. 13, No. 6, p. e0198048.

Čarnogurská, M., Příhoda, M. and Širillová, L., 2014. "Power losses and the efficiency of industrially used gearboxes". In *AIP Conference Proceedings*. American Institute of Physics, Vol. 1608, pp. 16–21.

Davies, T., 2006. "Freedom and constraint in coupling networks". *Proceedings of the Institution of Mechanical Engineers, Part C: Journal of Mechanical Engineering Science*, Vol. 220, No. 7, pp. 989–1010.

Glover, J.H., 1965. "Efficiency and speed-ratio formulas for planetary gear systems". *Prod. Eng.(NY)*, Vol. 27, pp. 72–79.

Hunt, K.H., 1978. *Kinematic geometry of mechanisms*, Vol. 7. Oxford University Press, USA.

Laus, L., Simas, H. and Martins, D., 2012. "Efficiency of gear trains determined using graph and screw theories". *Mechanism and Machine Theory*, Vol. 52, pp. 296–325.

Laus, L.P., 2011. *Machine efficiency determination using graph and screw theories : application to gear trains and parallel robots*. Doctoral degree thesis, Universidade Federal de Santa Catarina – UFSC, Florianópolis, SC.

Pathak, S., Jain, N. and Palani, I., 2016. "Investigations on surface quality, surface integrity and specific energy consumption in finishing of straight bevel gears by pech process". *The International Journal of Advanced Manufacturing Technology*, Vol. 85, No. 9, pp. 2207–2222.

Souza, M.B.d., 2022. *Powertrain optimization of hybrid and electric vehicles*. Ph.D. thesis, Graduate Program in Mechanical Engineering, Federal University of Santa Catarina, Florianópolis, Brasil.

Souza, M.B.d., Vieira, R.d.S., Martins, D., Cazangi, H.R. and Laus, L.P., 2017. "Mechanical efficiency determination of a dedicated hybrid transmisssion using graph and screw theories: a case study". In *24th ABCM International Congress of Mechanical Engineering (COBEM 2017)*. ABCM. doi:10.26678/ABCM.COBEM2017.COB17-0405.

Stockman, K., Dereyne, S., Defreyne, P., Algoet, E. and Derammelaere, S., 2015. "Efficiency measurement campaign on gearboxes". In *Energy efficiency in motor driven systems, Proceedings*. EEMODS, p. 11.

7. RESPONSIBILITY NOTICE

The authors are solely responsible for the printed material included in this paper.